applied optics

Statistical properties of dynamic speckles in application to laser focusing systems

ZHAN YU,[1,2] JIN GUO,[1] LISHENG LIU,[1] TINGFENG WANG,[1] AND YUANYANG LI[1,*]

[1]State Key Laboratory of Laser Interaction with Matter, Changchun Institute of Optics, Fine Mechanics and Physics, Chinese Academy of Sciences, Changchun, Jilin 130033, China
[2]University of Chinese Academy of Sciences, Beijing 100049, China
*Corresponding author: liyuanyang1108@163.com

Received 11 December 2018; revised 22 March 2019; accepted 22 March 2019; posted 22 March 2019 (Doc. ID 355093); published 19 April 2019

Dynamic speckles, which carry information about beam parameters of a diffuse object, are produced by a moving diffuse object under illumination of a Gaussian beam. In this paper, we consider that the diffuse object moves in a plane with constant velocity and discuss the statistical properties of dynamic speckles for estimating the variation of focusing spot size. The space–time statistical properties of dynamic speckle have been revealed by analyzing the space–time cross-correlation function of speckle intensity fluctuations detected at two points in the receiving plane. We discuss the influence of the distance between two point detectors on the detection results by simulation analyses, and the theoretical analysis results are verified by experiment. This method, which applies feedback of the dynamic speckle fields for estimating the variation of focusing spot size, will help a laser focusing system optimize focusing performance.

https://doi.org/10.1364/AO.58.003310

1. INTRODUCTION

It is well known that a diffuse object that is illuminated with laser beam generates a grain-like distribution of scattered light field. The scattered light field in this situation is called the speckle field [1]. The speckle field becomes available for researchers because the reflected speckle field carries the information about the laser beam parameters of the diffuse object. Based on Goodman's theory [2] the average speckle size of the fully developed speckle field is an inverse property of the speckle field, which can provide metrics for estimating the laser beam that concentrates on the remote rough target surface. With the study of second order statistical property of the received speckle field, some beam quality metrics [3–6], which are obtained by analyzing the statistical properties of the received speckle, have been introduced, and these methods can estimate the variation of the far-field focusing spot size. For example, these methods include the changes of power in the bucket [5] and variance of reflected speckle, the clipped speckle autocorrelation [4] metric, the clipped speckle edge integration [3] metric, and the speckle pattern sequential extraction [6] metric. But these methods only can be applied on a diffuse object in a stationary state.

The speckle pattern varies when the diffuse object moves, and it becomes dynamic at this moment. These dynamic speckles contain information about the velocity of the moving object, distance to the object surface, and width of the beam illuminating the object. The theoretical basis of the dynamic speckles [7] is established on the theory of Anisimov and many other scientists in which the dynamic speckles could be described by a space–time correlation function. Takai *et al.* [8] have theoretically investigated the dynamic speckles' statistical properties of time-varying speckles which are produced in the far-field diffraction region from a diffuse object moving in an arbitrary direction of three-dimensional space. The study reveals that the autocorrelation function of the speckle intensity fluctuation depends on the object's moving velocity, the waist width, and the wavelength of the illuminating Gaussian beam. Then, Takai *et al.* [9] have studied the translational and boiling motions of dynamic speckles produced in the Fresnel diffraction field under illumination of a Gaussian beam. They analyze the speckle motion from the space–time cross-correlation function of speckle intensity fluctuations detected at the two points in the receiving plane. The research is an analysis of translational and boiling motions of dynamic speckles produced from the translational motion of the diffuse object, and it shows that the correlation distance of time-varying speckle intensity fluctuations is determined by the waist radius of the illuminating Gaussian beam.

With further study on the statistical characteristics of dynamic speckle, there are some applications of dynamic speckles to metrology, such as applying dynamic speckles' statistical properties to measure the velocity [10–12] of moving diffuse objects and applying statistics of dynamic speckles for distance measurements [13,14]. In this paper, we used a space–time cross-correlation function of the dynamic speckle intensity fluctuation to analyze the statistical properties of dynamic speckles, and we propose a dual-detector cross-correlation method for estimating the far-field focus spot size. Then, we demonstrate that this method can be implemented in the laser focusing system to optimize the focusing performance of the system. At the same time, we discussed the influence of the distance between two detectors on the detection results. To the best of the authors' knowledge, this is the first paper to analyze focus spot size by a cross-correlation function of the dynamic speckle field. The feasibility of this method is verified by simulation analysis.

2. STATISTICAL PROPERTIES OF DYNAMIC SPECKLES

In this paper, we use the spatial and temporal properties of dynamic speckles to estimate the size of the focusing spot. The statistical properties of dynamic speckles have been revealed by analyzing the space–time cross-correlation function of speckle intensity fluctuations, which are detected at the two points in the receiving plane. The coordinate system for estimating the far-field laser spot size by using the statistical properties of dynamic speckles is as shown in Fig. 1. The dynamic speckles are produced by a moving diffuse object (η, ξ) with constant velocity ($\mathbf{V}$) under illumination of a Gaussian beam. The distance from the beam waist to the diffuse object and observation plane are z and R_0, respectively. And the distance between the diffuse object and the observation plane is R. According to the coordinate system shown in Fig. 1, the optical field distribution of light emerging from the diffuse object may be written as

$$U_0(\boldsymbol{\rho}, t) = E(\boldsymbol{\rho}) \exp[i\varphi(\boldsymbol{\rho} - \mathbf{V}t)] \exp(-2\pi i v t), \tag{1}$$

where $\boldsymbol{\rho} = (\xi, \eta)$, $E(\boldsymbol{\rho})$ is the amplitude distribution of the illuminating light, v is the frequency of the illuminating field, and $\phi(\boldsymbol{\rho})$ is the phase variation due to the random phase screen. In the observation plane $\mathbf{r} = (x, y)$, we need a Fresnel diffraction integral to calculate the amplitude distribution of the speckle field, and it is given by

$$U(\mathbf{r}, t) = \int U_0(\boldsymbol{\rho}, t) K(\boldsymbol{\rho}, \mathbf{r}) \mathrm{d}\rho, \tag{2}$$

where $K(\boldsymbol{\rho}, \mathbf{r})$ is the propagation function of the optical field from the diffuse object plane to the observation plane. The speckle intensity is a random variable depending on space and time, and its detection at the point $\mathbf{r}$ is denoted by

$$I(\mathbf{r}, t) = |U(\mathbf{r}, t)|^2. \tag{3}$$

The space–time cross-correlation function of the speckle-intensity variation $I(\mathbf{r}, t)$ can be studied from that of the speckle-intensity fluctuation defined by

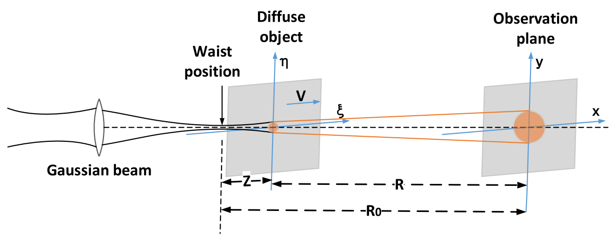

Fig. 1. Coordinate system of dynamic speckles.

$$\Delta I(\mathbf{r}, t) = I(\mathbf{r}, t) - \langle I(\mathbf{r}, t) \rangle. \tag{4}$$

If the receiving speckle field is a fully developed one, the real and imaginary parts of $U(\mathbf{r}, t)$ are independent of each other, and the correlation function of the intensity fluctuation is expressed by using the second-order correlation with respect to the complex amplitude [15] and is given by

$$\langle \Delta I(\mathbf{r}_1, t_1) \Delta I(\mathbf{r}_2, t_2) \rangle = |\langle U(\mathbf{r}_1, t_1) U^*(\mathbf{r}_2, t_2) \rangle|^2. \tag{5}$$

Based on Eqs. (1) and (2), the space–time correlation function of the $U(\mathbf{r}, t)$ can be obtained:

$$\begin{aligned} \Gamma(\mathbf{r}_1, \mathbf{r}_2; t_1, t_2) &= \langle U(\mathbf{r}_1, t_1) U^*(\mathbf{r}_2, t_2) \rangle \\ &= \iint E(\boldsymbol{\rho}_1) E(\boldsymbol{\rho}_2) \\ &\quad \times \langle \exp\{i[\varphi(\boldsymbol{\rho}_1 - \mathbf{V}t_1) - \varphi(\boldsymbol{\rho}_2 - \mathbf{V}t_2)]\} \rangle \\ &\quad \times K(\boldsymbol{\rho}_1, \mathbf{r}_1) K^*(\boldsymbol{\rho}_2, \mathbf{r}_2) \mathrm{d}\rho_1 \mathrm{d}\rho_2. \end{aligned} \tag{6}$$

If the roughness of the diffuse object surface is very large, and the variation of the random phase $\phi(\boldsymbol{\rho})$ is sufficient, we can obtain the following relation by

$$\langle \exp\{i[\varphi(\boldsymbol{\rho}_1) - \varphi(\boldsymbol{\rho}_2)]\} \rangle = \begin{cases} 1; & |\rho_1 - \rho_2| < \sqrt{\Delta S} \\ 0; & |\rho_1 - \rho_2| \geq \sqrt{\Delta S} \end{cases}, \tag{7}$$

where ΔS is the correlation area of the random phase $\phi(\boldsymbol{\rho})$. If the correlation area ΔS is sufficiently small compared with the extents of the illuminating light $E(\boldsymbol{\rho})$ over the diffuse object and the propagation function $K(\boldsymbol{\rho}, \mathbf{r})$, Equation (6) can be turned into

$$\begin{aligned} \Gamma(\mathbf{r}_1, \mathbf{r}_2; \tau) = \Delta S \int & E\left(\boldsymbol{\rho} - \frac{\mathbf{V}}{2}\tau\right) E^*\left(\boldsymbol{\rho} + \frac{\mathbf{V}}{2}\tau\right) \\ & \times K\left(\boldsymbol{\rho} - \frac{\mathbf{V}}{2}\tau, \mathbf{r}_1\right) K\left(\boldsymbol{\rho} + \frac{\mathbf{V}}{2}\tau, \mathbf{r}_2\right) \mathrm{d}\rho, \end{aligned} \tag{8}$$

where $\tau = t_2 - t_1$, and Eq. (8) is the assumption about the temporal stationary of dynamic speckles. According to Eqs. (5) and (6), the square of the space–time correlation function of the speckle field reflects the statistical information of the speckle intensity fluctuation. The normalized space–time cross-correlation function of time-varying speckle intensity fluctuations is given by

$$\begin{aligned} \gamma_{\Delta I}(\mathbf{X}, \tau) &= |\Gamma(\mathbf{r}_1, \mathbf{r}_2; \tau)|^2 / |\Gamma(0, 0; 0)|^2 \\ &= \frac{\left| \int E\left(\boldsymbol{\rho} - \frac{\mathbf{V}}{2}\tau\right) E^*\left(\boldsymbol{\rho} + \frac{\mathbf{V}}{2}\tau\right) \times \exp\left[i\frac{2\pi}{\lambda R}(\mathbf{X} - \mathbf{V}\tau)\boldsymbol{\rho}\right] \mathrm{d}\rho \right|^2}{\left| \int |E(\boldsymbol{\rho})|^2 \mathrm{d}\rho \right|^2}, \end{aligned} \tag{9}$$

where $\mathbf{X} = \mathbf{r}_1 - \mathbf{r}_2$. From Eq. (9), we can find that the speckle field is spatially stationary, depending only on the space variable $\mathbf{X}$.

When a Gaussian beam with a waist width ω_0 is employed to illuminate the diffuse object, the amplitude distribution $E(\boldsymbol{\rho})$ is given by

$$E(\boldsymbol{\rho}) = \frac{\omega_0}{\omega} \exp(2i\pi z/\lambda) \exp(-|\boldsymbol{\rho}|^2/\omega^2) \exp(i\pi|\boldsymbol{\rho}|^2/\lambda Q), \tag{10}$$

where ω and Q are the width and wavefront-curvature radius of the illuminating beam at the diffuse object. The two parameters ω and Q are given by

$$\omega = \omega_0(1 + z^2/a^2)^{1/2}, \tag{11}$$

$$Q = z(1 + a^2/z^2), \tag{12}$$

where

$$a = \pi\omega_0^2/\lambda. \tag{13}$$

Taking Eq. (10) into Eq. (9), we can obtain

$$\gamma_{\Delta I}(\mathbf{X}, \tau) = \exp(-|\mathbf{V}|^2\tau^2/\omega^2) \times \exp\left[-\left|\mathbf{X} - \left(1 + \frac{R}{Q}\right)\mathbf{V}\tau\right|^2/\Delta x^2\right], \tag{14}$$

where Δx corresponds to the average grain size of speckles and is defined by

$$\Delta x = \frac{\lambda R}{\pi\omega}. \tag{15}$$

In order to further discuss the properties of dynamic speckles, the time correlation length τ_c of the time-varying speckle intensity fluctuations is introduced:

$$\tau_c = \frac{1}{|\mathbf{V}|}\left[\frac{1}{\omega^2} + \frac{(1 + R/Q)^2}{\Delta x^2}\right]^{-1/2}. \tag{16}$$

We use τ_c to express Eq. (14); the $\gamma_{\Delta I}$ can be given as

$$\gamma_{\Delta I} = \exp\left(-\frac{|\mathbf{X}|^2}{X_c^2}\right)\exp\left[-\frac{(\tau - \tau_d)^2}{\tau_c^2}\right], \tag{17}$$

where

$$\tau_d = \tau_c^2(1 + R/Q)\mathbf{V}\mathbf{X}/\Delta x^2, \tag{18}$$

$$X_c = \left[\frac{\Delta x^2 + (1 + R/Q)^2\omega^2}{1 + (1 + R/Q)^2\omega^2\sin^2\theta/\Delta x^2}\right]^{1/2}, \tag{19}$$

and θ is the angle between the vectors of V and X. Equation (18) indicates the time delay τ_d of the cross-correlation function of speckle intensities which are detected at the two points $\mathbf{r}_1$ and $\mathbf{r}_2$ with the vector distance X. Equation (19) represents that the cross-correlation peak becomes e^{-1} at time $\tau = \tau_d$ for the two detecting points distance $|\mathbf{X}| = X_c$. The maximum value of X_c is given for $\theta = 0$ in which the two points are situated in the velocity direction of the moving object. In this paper, we consider that the distance vector between the two detecting points is parallel to the velocity vector. In this case, Eq. (19) can be conveniently rewritten as

$$X_c = \left[\Delta x^2 + \left(1 + \frac{R}{Q}\right)^2\omega^2\right]^{1/2}. \tag{20}$$

By substituting Eqs. (11), (12), (13), and (15) into Eq. (20) and using the relation $R = R_0 - z$, where R_0 is the distance from the beam waist position to the receiving plane, the X_c is given by

$$X_c = \omega_0(1 + R_0^2/a^2)^{1/2} = \omega_0[1 + (\lambda R_0/\pi\omega_0^2)^2]^{1/2}. \tag{21}$$

The cross-correlation peak of two detection points with a distance of $|X|$ is located at $T = T_d$. In this time, the value of Eq. (17) is given by

$$\gamma_{\Delta I} = \exp\left(-\frac{|\mathbf{X}|^2}{X_c^2}\right). \tag{22}$$

3. METHOD TO ESTIMATING THE FAR-FIELD LASER BEAM BY USING DYNAMIC SPECKLES

In this paper, we propose a method of using dynamic statistical properties of laser speckles to estimate the size of the far-field laser beam. Compared with the telescope system, which directly observes the size of far-field laser beam, this method has higher detection accuracy. At this time, we consider that the distance between the diffuse object and the observation plane is much larger than the distance from the beam waist to the diffuse object; we can get $R \gg z$ in the dynamic speckles coordinate system of Fig. 1. Based on this condition, we further study the time delay τ_d of the cross-correlation function of speckle intensities detected at the two points $\mathbf{r}_1$ and $\mathbf{r}_2$ with the vector distance $|\mathbf{X}|$. Taking Eq. (16) into Eq. (18), we can obtain

$$\tau_d = \frac{\mathbf{X}}{\mathbf{V}}\frac{\left(1 + \frac{R}{Q}\right)}{\frac{\Delta x^2}{\omega^2} + \left(1 + \frac{R}{Q}\right)^2} = \frac{\mathbf{X}}{\mathbf{V}}\frac{1}{\frac{\lambda^2R^2}{\pi^2\omega^4F} + F}, \tag{23}$$

where $F = 1 + R/Q$. From Eq. (23), we can see that $\tau_d(F) = -\tau_d(-F)$, and in this paper we only discuss $F > 0$ to get the relationship between the time delay τ_d of the cross-correlation function and the width ω of the illuminating beam at the diffuse object. If we do not consider the effect of laser beam size ω, F can be seen as a function of τ_d. (a) When $0 < F < (\lambda R)/(\pi\omega^2)$, the time delay τ_d of the cross-correlation function increases as F increases. (b) When $F > (\lambda R)/(\pi\omega^2)$, the time delay τ_d of the cross-correlation function decreases as F increases. According to the above conditions, the following results can be obtained from Eq. (23):

(1) For $z \gg a$, there is $R \gg z \approx Q$ and $F = 1 + R/z > (\lambda R)/(\pi\omega^2)$.

When the width of laser beam ω increases with the distance from the beam waist to the diffuse object z, the value of F decreases, and we can obtain that the time delay τ_d of the cross-correlation function increases.

(2) For $z \ll a$, according to Eq. (11), we can obtain that $\omega \approx \omega_0$, $F = 1 + R/Q \approx 1 + zR/a^2$.

When the width of laser beam ω increases with the waist width ω_0 of the Gaussian beam, the distance from the beam waist to diffuse object z decreases and the value of F decreases. Taking Eq. (12) into Eq. (23), τ_d is given by:

$$\tau_d = \frac{\mathbf{X}}{\mathbf{V}}\frac{1}{\frac{\lambda^2R^2(a^2+z^2)}{\pi^2\omega^4(Rz+a^2+z^2)} + F} = \frac{\mathbf{X}}{\mathbf{V}}\frac{1}{\frac{\lambda^2R^2\pi a\omega^2/\lambda}{\pi^2\omega^4[Rz+\pi a\omega^2/\lambda]} + F}$$
$$= \frac{\mathbf{X}}{\mathbf{V}}\frac{1}{\frac{\lambda^2R^2a}{\pi\omega^2(Rz\lambda+\pi a\omega^2)} + F} = \frac{\mathbf{X}}{\mathbf{V}}\frac{1}{\frac{\lambda^2R^2}{\pi\omega^2\left(R\frac{z}{a}\lambda+\pi\omega^2\right)} + F}. \tag{24}$$

According to Eq. (24), when the width of laser beam ω increases and the value of F decreases, the time delay τ_d of the cross-correlation function increases.

(3) For other conditions, when the distance z between the beam waist and the diffuse object increases, the curvature radius Q of the illuminating beam increases and the value of F decreases. From Eq. (24), we can find that when the width of laser beam ω increases, the time delay τ_d increases.

Based on these results, we can conclude that the time delay increases with the width of the illuminating beam at the diffuse object.

4. SIMULATION RESULTS

This section introduces the simulation process for estimating the size variation of far-field spot by using dynamic speckle statistical properties and makes a simple analysis of the simulation results. The optical layout of the setup is shown in Fig. 1. A 532 nm collimated laser beam is focused by the lens to the moving diffraction target. The lens is used for adjusting the size of the laser spot on the moving object. Using the lens formula for Gaussian beams [16], we can estimate the size of the laser spot on the objects. Supposing that the Gaussian laser beam has a waist width ω_1, the distance between the laser collimator and the lens is L_1, and the distance between the lens and the laser spot on the objects is L_2, then the radius ω of the spot on the moving objects can be calculated by using

$$\omega = \omega_0 \left[1 + \left(\frac{\lambda z}{\pi \omega_0^2} \right)^2 \right]^{1/2}, \tag{25}$$

where

$$\omega_0^2 = \frac{f^2 \omega_1^2}{(f - L_1)^2 + \left(\frac{\pi \omega_1^2}{\lambda} \right)^2}, \tag{26}$$

$$z = L_2 - \left[f + \frac{(L_1 - f) f^2}{(L_1 - f)^2 + \left(\frac{\pi \omega_1^2}{\lambda} \right)^2} \right], \tag{27}$$

with f as the focal length of the lens. In the simulation of a dynamic speckle pattern that evolves with time, we calculate its time history by considering only the movement of the scatterers. Therefore, in this paper the movement of the scatterers model [17] is used to simulate dynamic speckles. The schematic setup of the simulation model is illustrated in Fig. 2. In the movement of the scatterers model, the diffuse target surface is divided into N sampling points, and each sampling point is established by random phase distributions which are randomly generated from 0 to 2π to obtain a set of phase screens. We assume the random phase of the ith sampling point is ϕ_i, the distance from the sampling point to the detector 1 is R_{1i}, and the distance from the detector 2 is R_{2i}. The distribution of the light field received by the two detectors can be obtained by superposition of the light field generated by each scattering sample:

$$U_{1t} = \sum_i \frac{Ai}{R_{1i}} \exp(jkR_{1i} + \varphi_i), \tag{28}$$

$$U_{2t} = \sum_i \frac{A_i}{R_{2i}} \exp(jkR_{2i} + \varphi_i), \tag{29}$$

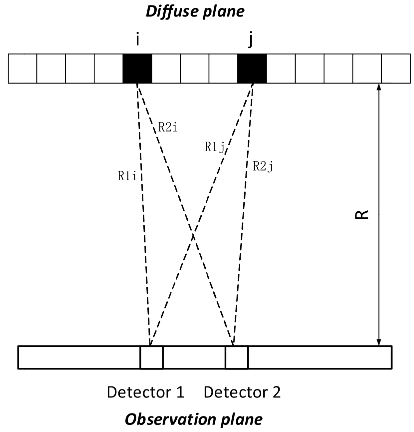

Fig. 2. Schematic setup of simulation model for detecting echo speckle intensities using two point detectors.

where A_i is the amplitude of the focused light field at the ith sample point on the diffuse target.

According to the principle of the movement of the scatterers model, it is only necessary to sample the rough surface in the simulation, and the receiving plane does not need to be sampled. Therefore, it can make the sampling interval of the diffuse plane smaller, and continuous motion of the speckles can be obtained.

In the simulation, the distance between the laser collimator and the lens is $L_1 = 0$ m, and the distance between the lens and the laser spot on the diffuse object is $L_2 = 100$ m. We obtain different sizes of focusing spots on the moving object by changing the waist width ω_1 of the Gaussian laser beam and the focal length of the lens f. In this paper, we use a square matrix of dimension $N * N$ to describe the light field of the diffuse plane and $N = 100$. The sampling interval in the light field is $4\omega/N$, ω is the radius of spot on the moving object, the wavelength is $\lambda = 0.532$ μm, and the observation plane is 100 m far from the diffuse plane ($R = 100$ m). The diffuse target motion speed is $|\mathbf{V}| = 1$ m/s.

Figure 3 shows the time-varying speckle-intensity fluctuation received by two detectors using the movement of the scatterers method. The radius of the spot on the moving objects is 0.58 mm, and the distance between two detectors is 20 mm. It can be seen from Fig. 3 that there is a certain correlation delay between the signals received by the two detectors. The cross-correlation rule of the dual detector uses this correlation delay to detect the size of the focusing spot on the moving target.

Figure 4 is the simulation result of the normalized space–time cross-correlation function. Figure 4(a) shows the simulation results obtained by single sampling, and Fig. 4(b) shows the simulation results obtained after 15 samplings. The radius ω of the spot on the moving objects is 0.46 mm. It can be seen from Fig. 4(a) that the correlation peak is not fully highlighted because the sampling points are insufficient, which leads to the deviations on the estimated results of the cross-correlation function. In fact, a large number of sampling points will increase the sampling time and affect the real-time detection of the variation of the focusing spot size. In this paper, the above problem is

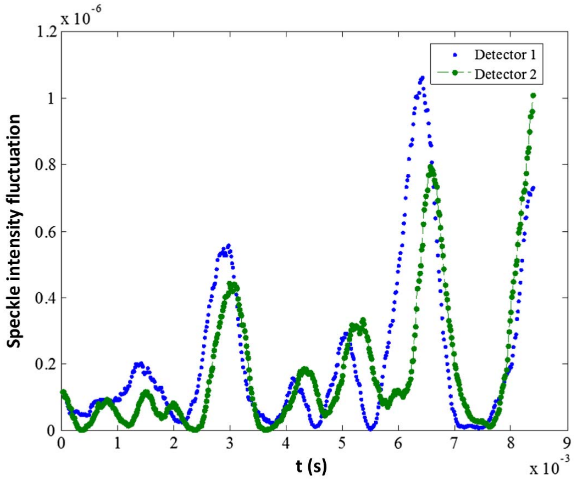

Fig. 3. Speckle-intensity fluctuation received by two detectors.

solved by using the method of averaging the results obtained from the multiple samplings. The specific method is as follows. In the simulation, the echo signal is sampled many times, and the cross-correlation function is calculated using fewer sampling points each time. Then take the average of the results of multiple sets of cross-correlation functions. A visible correlation peak can be seen in Fig. 4(b), which can be verify that the above method can enhance the detection ability of the correlation peak.

Figure 5 shows the simulation results of the dynamic speckles' normalized space–time cross-correlation function received by the observation system, and the different focal spot sizes are obtained in the simulation by changing the focal length of the focusing system. With the increases of size of the focal spot, the time delay of the correlation peak also increases; this phenomenon is consistent with the results obtained by the theoretical derivation. The simulation results verify the feasibility of the dual-detector cross-correlation method for estimating the size variation of the far-field focal spot.

Figure 6 shows the simulation results of the dynamic speckles' normalized space–time cross-correlation function of two point detectors at different distances; the spot sizes at the surface of the moving target are 0.423, 0.585, and 0.996 mm. It can be seen from the figure, when the distance $|\mathbf{X}|$ between two point detectors increases, the correlation peak delay of the cross-correlation function also increases; this result is consistent with formulas (23) and (24). According to this phenomenon,

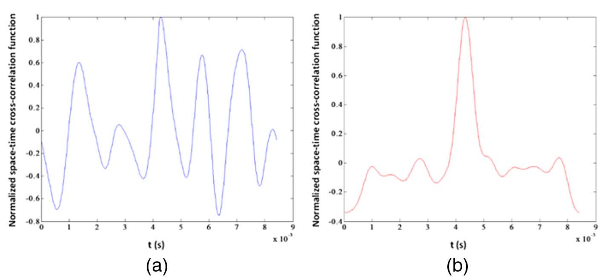

Fig. 4. Normalized space–time cross-correlation function of the received speckles.

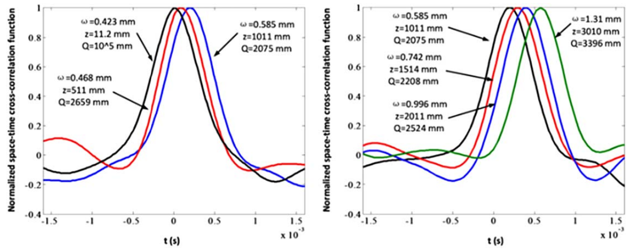

Fig. 5. Simulation results of the dynamic speckle normalized space–time cross-correlation function, where the distance between two detectors $|\mathbf{X}| = 20$ mm.

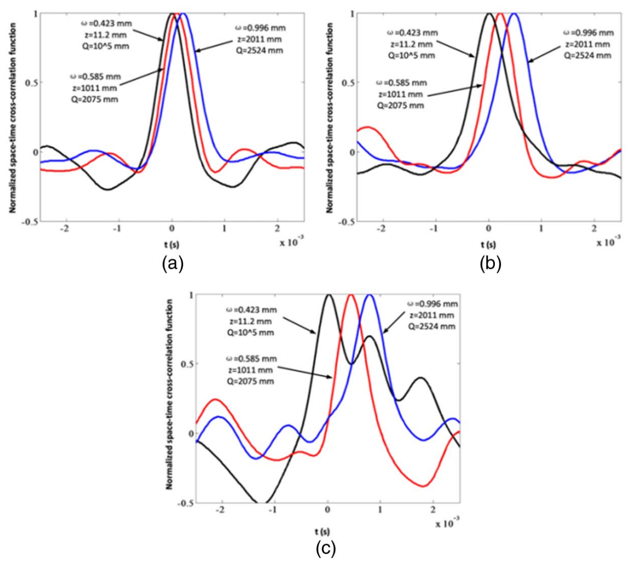

Fig. 6. Simulation results of the dynamic speckles normalized space–time cross-correlation function, where the distance between two detectors is (a) $|\mathbf{X}| = 10$ mm, (b) $|\mathbf{X}| = 25$ mm, (c) $|\mathbf{X}| = 40$ mm.

when the dual-detector cross-correlation method is used to estimate the far-field focusing spot size, the measurement accuracy can be improved by increasing the distance $|\mathbf{X}|$ between two point detectors. According to Eq. (22), the value of the correlation peak decreases when the distance between two detectors increases. When $|\mathbf{X}|$ is large enough, the correlation peak is submerged in the received signal, resulting in the failure of the dual detector cross-correlation method. It can be seen from Fig. 6(c) that the relative intensity of the correlation peaks is significantly reduced. Equation (19) represents that the cross-correlation peak becomes e^{-1} at time $\tau = \tau_d$ for the two detecting points at distance $|\mathbf{X}| = X_c$. In order to avoid the correlation peak to be submerged in the deviation of the estimated cross-correlation function, the distance between the two detectors should be less than X_c:

$$|\mathbf{X}| < X_c = \omega_0[1 + (\lambda R_0/\pi\omega_0^2)^2]^{1/2}. \quad \textbf{(30)}$$

5. EXPERIMENT

The experimental device for testing the feasibility of the correlation peak delay metric is shown in Fig. 7. In the experiment,

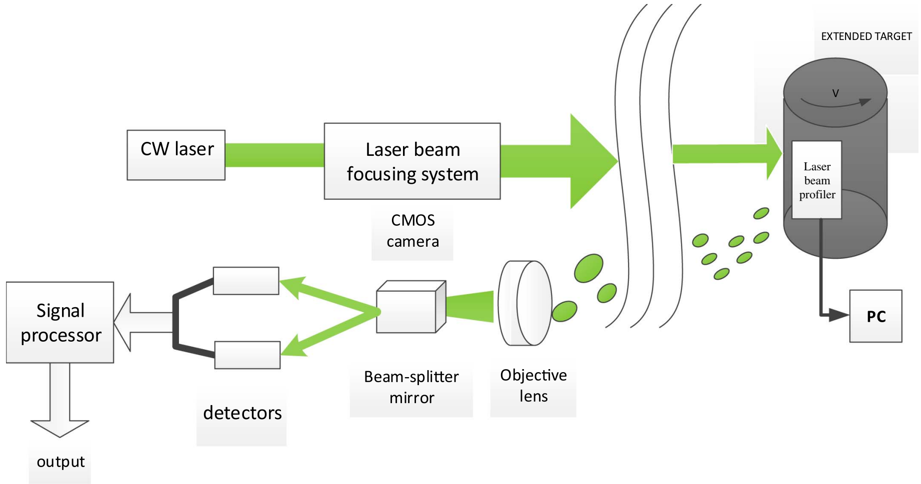

Fig. 7. Experimental device for testing the feasibility of the correlation peak delay metric.

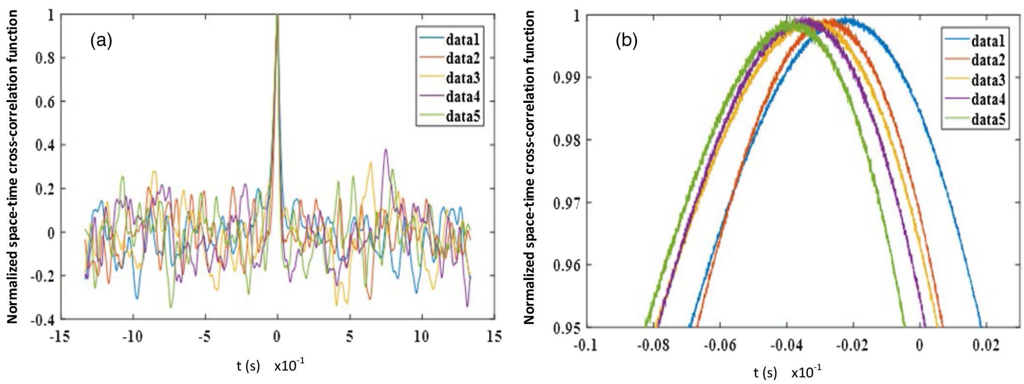

Fig. 8. Experimental results of the dynamic speckle normalized space–time cross-correlation function. (a) Initial output result of the cross-correlation function. (b) Result of enlarging (a). The sample rate is 10 MHz, and the corresponding spot size from data 1 to data 5 are 2.69, 2.73, 2.81, 2.89, and 2.99 mm.

we focus a continuous wave laser whose wavelength is 0.532 μm on a diffuse target, and the observation system collects the returned speckle field which is generated by the laser beam illuminating the diffuse target surface. The distance from the diffuse target to the observation system is 7.1 m. The observation system consists of a beamsplitter mirror and two point detectors. We change the focal length of the laser beam focusing system to obtain different sizes of focusing spot. Because of the parameters of the experimental system, the distance between the two detectors is very small (less than 1.5 mm), and we add a beamsplitter mirror between the positive lens and the detectors. The focal length of the positive lens is 800 mm, and the diameter of the lens is 70 mm. The laser beam profiler detection system directly gets the information of the focusing spot size on the target, which helps us verify the speckle metric performance. The signal processing system converts the received information of speckle field intensity fluctuations into speckle metric output. When the metric output is obtained, the laser beam profiler is applied to replace the diffuse target for obtaining the actual size of the corresponding focal spot, so that the experimental results can be verified and analyzed. In the experiment, we use the guide rail to calibrate the position of the focusing spot; this makes the laser beam profiler be in the same position as the spot.

The experimental results of the correlation peak delay metric are shown in Fig. 8. It can be seen from the experimental data that as the size of the focal spot increases, the time delay of the correlation peak also increases. This experimental result is consistent with the results obtained by the theoretical derivation.

6. CONCLUSION

The characteristic time scale of speckle intensity fluctuations is directly related to speckle dynamics, which are related to focal spot size on the surface of the moving target. In this paper, we propose a dual-detector cross-correlation method to estimate the focal spot size of a remote moving diffuse object. The relationship between the correlation peak delay and far-field focal spot size is derived according to the dynamic speckle space–time cross-correlation function. By the theoretical analysis, we can conclude that the time delay of correlation peak increases with the focal spot size on the remote moving diffuse object. Combined with theoretical analysis, the feasibility of the dual-detector cross-correlation method is verified by simulation analysis. Then we discuss the effect of the distance between two detectors on the measurement accuracy, and the selection rule of the distance is given according to Eq. (30). In this paper, the output of the metric is consistent with its theoretical analysis results, and the performance of the speckle metric is verified by experiments. This work provides the basis for applying dynamic speckles to monitor the variation of the far-field focusing beam width.

REFERENCES

1. B. Frieden, "Laser speckle and related phenomena," Optica **23**, 842–843 (2010).
2. J. W. Goodman and L. M. Narducci, "Statistical optics," Phys. Today **39**(10), 126 (1986).
3. M. A. Vorontsov and G. W. Carhart, "Target-in-the-loop adaptive optics: wavefront control in strong speckle-modulation conditions," Proc. SPIE **4825**, 67–74 (2002).
4. Y. Li, J. Guo, L. Liu, T. Wang, W. Tang, and Z. Jiang, "Clipped speckle autocorrelation metric for spot size characterization of focused beam on a diffuse target," Opt. Express **23**, 7424–7441 (2015).
5. G. Carhart, M. Gatz, M. Vorontsov, S. Lachinova, and T. Weyrauch, "Speckle-metric-optimization-based adaptive optics for laser beam projection and coherent beam combining," Opt. Lett. **37**, 2802–2804 (2012).
6. Z. Yu, Y. Li, L. Liu, J. Guo, T. Wang, and G. Yang, "Speckle pattern sequential extraction metric for estimating the focus spot size on a remote diffuse target," Appl. Opt. **56**, 8941–8949 (2017).
7. V. V. Anisimov, S. M. Kozel, and G. R. Lokshin, "Space-time statistical properties of coherent radiation scattered by a moving diffuse reflector," Opt. Spectrosc. **27**, 258 (1969).
8. N. Takai, T. Asakura, and T. Iwai, "Dynamic statistical properties of laser speckle produced by a moving diffuse object under illumination of a Gaussian beam," J. Opt. Soc. Am. **72**, 460–467 (1982).
9. N. Takai, T. Iwai, and T. Asakura, "Correlation distance of dynamic speckles," Appl. Opt. **22**, 170–177 (1983).
10. E. A. Moro, M. E. Briggs, and L. M. Hull, "Defining parametric dependencies for the correct interpretation of speckle dynamics in photon Doppler velocimetry," Appl. Opt. **52**, 8661–8669 (2013).
11. E. B. Flynn, E. A. Moro, M. E. Briggs, and W. J. Warren, "Simulating translation-induced laser speckle dynamics in photon Doppler velocimetry," Appl. Opt. **53**, 4661–4668 (2014).
12. E. A. Moro and M. E. Briggs, "Note: simultaneous measurement of transverse speed and axial velocity from a single optical beam," Rev. Sci. Instrum. **84**, 016110 (2013).
13. D. V. Semenov, E. Nippolainen, and A. A. Kamshilin, "Fast distance measurements by use of dynamic speckles," Opt. Lett. **30**, 248–250 (2005).
14. A. Kamshilin, D. V. Semenov, and E. Nippolainen, "Statistics of dynamic speckles in application to distance measurements," in *International Conference on Optics-Photonics Design & Fabrication* (2008).
15. T. Asakura and N. Takai, "Dynamic laser speckles and their application to velocity measurements of the diffuse object," Appl. Phys. A **25**, 179–194 (1981).
16. S. A. Self, "Focusing of spherical Gaussian beams," Appl. Opt. **22**, 658–661 (1983).
17. H. J. Rabal, R. Arizaga, N. L. Cap, E. Grumel, and M. Trivi, "Numerical model for dynamic speckle: an approach using the movement of the scatterers," J. Opt. A **5**, S381 (2003).